Circuits and Systems
Mekelweg 4,
2628 CD Delft
The Netherlands
http://ens.ewi.tudelft.nl/

CAS-2017-4512812

M.Sc. Thesis

Indoor Localization with Low Energy Bluetooth

Wangyang Yu

Abstract

Indoor localization is of great importance in our daily life. Different from GPS in outdoor environments, there is still no satisfactory system for indoor localization. There are many problems that need to be solved in indoor localization, for example, the effects of reverberations and obstacles.

This study develops an accurate indoor localization system. In this thesis, we use low energy Bluetooth signals for localization. The time difference of arrival measurements are obtained through the subtraction of time of arrival measurements. The time of arrival information of each receiver is measured with the generalized cross correlation with phase transform. With the time difference of arrival information, the localization is solved in a distributed way. Four proposed time-difference-of-arrival localization methods are compared. The optimal sensor geometry is also examined based on the Cramer-Rao lower bound. Experimental results show that we can localize the source with an accuracy of less than one centimeter when the SNR is higher than 5dB. Furthermore, the proposed indoor localization system is robust to multipath effects and non-line-of-sight sources. In addition, we examine how many sources we can accurately localize simultaneously in an indoor environment in the thesis.

Indoor Localization with Low Energy Bluetooth

THESIS

submitted in partial fulfillment of the
requirements for the degree of

MASTER OF SCIENCE

in

ELECTRICAL ENGINEERING

by

Wangyang Yu
born in Dandong, China

This work was performed in:

Circuits and Systems Group
Department of Microelectronics
Faculty of Electrical Engineering, Mathematics and Computer Science
Delft University of Technology

Delft University of Technology

DELFT UNIVERSITY OF TECHNOLOGY
DEPARTMENT OF
MICROELECTRONICS

The undersigned hereby certify that they have read and recommend to the Faculty of Electrical Engineering, Mathematics and Computer Science for acceptance a thesis entitled **"Indoor Localization with Low Energy Bluetooth"** by **Wangyang Yu** in partial fulfillment of the requirements for the degree of **Master of Science**.

Dated: May 3, 2017

Chairman: _____
dr.ir. Richard Heusdens, TU Delft

Advisor: _____
dr.ir. Richard Heusdens, TU Delft

Committee Members: _____
dr.ir. Gerard Janssen, TU Delft

_____
dr. Jan van Gemert, TU Delft

_____
dr. ir. Arash Noroozi, ELPANAV

Abstract

Indoor localization is of great importance in our daily life. Different from GPS in outdoor environments, there is still no satisfactory system for indoor localization. There are many problems that need to be solved in indoor localization, for example, the effects of reverberations and obstacles.

This study develops an accurate indoor localization system. In this thesis, we use low energy Bluetooth signals for localization. The time difference of arrival measurements are obtained through the subtraction of time of arrival measurements. The time of arrival information of each receiver is measured with the generalized cross correlation with phase transform. With the time difference of arrival information, the localization is solved in a distributed way. Four proposed time-difference-of-arrival localization methods are compared. The optimal sensor geometry is also examined based on the Cramer-Rao lower bound. Experimental results show that we can localize the source with an accuracy of less than one centimeter when the SNR is higher than 5dB. Furthermore, the proposed indoor localization system is robust to multipath effects and non-line-of-sight sources. In addition, we examine how many sources we can accurately localize simultaneously in an indoor environment in the thesis.

Acknowledgments

I would like to thank all of them who contribute to my master thesis.

First of all, I would like to thank my supervisor dr.ir. Richard Heusdens, who gives me the opportunity to do this project. I really appreciate for your time, support, valuable guidance, critical suggestions and encouragement. You are such a pleasant supervisor. I have learned a lot from you. Thanks, Richard.

I would like to express my gratitude for Arash Noroozi, who puts up this project. Thank you for all your help during my master thesis. Arash is so kind to give responses to all the inquiries. I have learned very much from you.

Moreover, I would like to thank my committee members, dr.ir. Gerard Janssen and dr. Jan van Gemert. Thank you for your time.

Finally, I am so grateful for my family and friends for the encouragement, support and company.

Wangyang Yu
Delft, The Netherlands
May 3, 2017

Contents

List of Figures

1 Introduction

Localization techniques are more and more important in every aspect of daily life. In many applications with multiple sensors, the relative sensor positions are required to be known. For example, in the hospital, the position of patients can be obtained by the medical staff if the patients take the sensors with them. In supermarkets, customers with sensors can be provided with specific sales information based on the current location. In outdoor environments, global positioning system (GPS) performs well and is widely used. However, GPS does not work well in the indoor environment because of many obstacles and line-of-sight is not guaranteed. Nowadays, diverse techniques for indoor localization are proposed, such as methods based on received signal strength (RSS), time-of-arrival (TOA), time-difference-of-arrival (TDOA), or angle-of-arrival (AOA). In most of these examples, the signals to be used for localization can vary from application to application. As an example, TOA measurements can be obtained from acoustical signals, WiFi signals or Bluetooth signals, each having its own characteristics.

TOA, TDOA, AOA and RSS are the most widely used indoor localization techniques. TOA based techniques estimate the location of the source through the intersection of the range of the receivers. The range information can be obtained from the TOA measurements by multiplying them with the propagation speed of the signals used to measure the TOAs [1]. TOA based techniques can be used in indoor environments because they are robust against multipath effects. However, TOA based techniques have to deal with the unknown onset time, the time that the signals are generated, and the unknown internal delay, the time that the receiver uses to register the signal as received after the signal reaches the receiver [2]. In order to obtain accurate TOA measurements, precise synchronization is required among transmitters and receivers [1]. There are several TOA based algorithms for localization, such as, multidimensional scaling (MDS) [3], maximum likelihood algorithm (MLS) [1] and singular value decomposition (SVD)-based approach [2]. Different from TOA based techniques, TDOA based techniques use the time differences of arrival between several receivers to locate the sources. TDOA often uses the generalized cross correlation of the received signals to compute the TDOAs. In order to compute the generalized cross correlation, the receivers must have a data link between each other to share the received signals, which requires large bandwidth and power consumption [4]. Since the difference of arrival times is used for localization, only the receivers are required to be synchronized and there is no need to eliminate the effect of the unknown onset time. Similar to TOA based techniques, TDOA based techniques are robust against multipath effects [5]. In addition, TDOA based techniques can obtain the same accuracy as TOA based techniques [6].

Alternatively, angle information or received signal strength can be used for localization. The basic principle of AOA is that the intersection between the angles of received signals can locate the sensors [1]. AOA based techniques are not always considered for localization

because they require large dimensions of directional antennas. The advantage of AOA based techniques is that they are robust to the large scale fading [7]. On the other hand, RSS based techniques are always connected with fingerprints [8]. The cost is low and most receivers can estimate the received signal strength. Nevertheless, the accuracy is relative low since the strength of the received signals is sensitive to noise and interferers [1]. Several algorithms exist for RSS based localization, like the K-nearest neighbors (KNN) scheme, support vector machines (SVM) [9], principle component analysis (PCA), multiple discriminant analysis (MDA) and dynamic hybrid projection (DHP) [10].

The above mentioned localization methods are based on measurements obtained from certain signals. For that purpose, different types of signals can be used. The use of ultrasound signals leads to good accuracy for indoor localization (less than one meter) [11]. In addition, ultrasound signals are robust to the effects of indoor obstructions because the wave length is relatively long. However, the disadvantage is that the environmental temperature will influence the speed of ultrasound signals significantly [12]. Alternatively, we can use ultra-wide bandwidth (UWB) signals. Because of the large bandwidth, UWB signals are robust to propagation fading. Moreover, interferences can be rejected and accurate ranging can be achieved [13]. The backside is that when we use UWB signals for localization, the cost of the corresponding equipments is relatively high [14]. Other than ultrasound and UWB signals, radio frequency identification (RFID) is frequently used for localization. RFID uses the electromagnetic transmission to a radio frequency circuit to store and retrieve data [15]. The advantage is that RFID has no requirement on line-of-sight because it can penetrate solid objects except for mentals. However, the absorption, the reflection and the coverage of RF signals limit the use of RFID for indoor localization [12]. Another widely used wireless technology in localization is infrared (IR). There is no radio electromagnetic interference with IR technology. However, it requires line-of-sight and the cost of system hardware and maintenance is relatively high [12]. Besides these signals, Wi-Fi is widely used in indoor localization. The popularity of using Wi-Fi signals is mainly because almost every indoor environment has the corresponding infrastructure and every mobile device has the corresponding receiver, which can save a lot of money for extra installation. Nevertheless, when Wi-Fi is used for RSS based localization techniques, the accuracy is limited because the signals are sensitive to the presence of people and small objects [16]. Last but not least, similar to Wi-Fi, Bluetooth signals draw attention to the localization as well. However, since mobile devices are small and the power of batteries is constrained, Bluetooth signals suit mobile devices better than Wi-Fi signals due to limited power consumption [17]. In particular, Bluetooth low energy (BLE), a subset of the latest core version of Bluetooth, can reduce the classic Bluetooth's power consumption [18]. In addition, Bluetooth can choose frequency hopping spread spectrum (FHSS) as the transmission scheme, which can significantly reduce the effect of interferences [19]. Bluetooth is a highly accepted standard and there are billions of Bluetooth devices around the world. In addition, Bluetooth is getting to be established as one of the main foundations of the Internet of things (IoT) [20]. Although Bluetooth signals are popular around the world, they are not widely used in indoor localization. Many people hold the opinion that Bluetooth signals cannot be used for localization because of limited accuracy [21].

1.1 Problem Definition and Outline

The work presented in this thesis is a cooperation between TU Delft and the company ELPANAV. ELPANAV is interested in localization using Bluetooth signals in indoor environments. The set-up we will consider in this thesis is described here. The sources broadcast Bluetooth signals periodically. We assume the receivers are synchronized precisely, but not synchronized with the transmitters. Moreover, the positions of the receivers are assumed to be known beforehand. As a consequence, we will use TDOA based techniques to locate the sources in indoor environments. In the thesis, the image method is used to simulate the communication channel in indoor environments [22].

In the thesis, the following questions are addressed. Given the set-up described above,

- How can we use TDOA measurements for localization?
- How accurate can we locate the sources with TDOA measurements?
- How can we implement the localization methods in a distributed way?
- What is the optimal sensor geometry?
- How to deal with problems like multipath and non-line-of-sight?
- How many sources can we accurately localize simultaneously in an indoor environment?

This thesis is organized as follows. Chapter 2 is about the TDOA measurements. In Chapter 3, we discuss TDOA based localization techniques, where centralized methods and decentralized methods are included. In addition, we present the Cramer-Rao lower bound of TDOA based localization and the optimal sensor geometry. We will analyze the practical aspects in Chapter 4, like multipath effects, the absence of line-of-sight, etc. At the end, in Chapter 5, we draw conclusions and address further works.

Time Difference of Arrival Measurement

2

As mentioned in the introduction, we will use TDOA based localization. Before localization, we must have access to the TDOA measurements. There are two ways for computing the TDOA measurements. The first method is that the receivers calculate the cross correlation between the received signals and compute the TDOA measurement by finding the peak of the cross correlation function. However, this requires the receivers to transmit signals between each other, which is not applicable to the project at hand because with low energy Bluetooth, the receivers can only transmit a small quatity of data, like a TOA measurement, instead of a complete signal [18]. We therefore, use an alternative method, which is based on the subtraction of the TOA measurements between receivers. Each receiver stores a segment of the Bluetooth signal as the reference signal. The receivers calculate the cross correlation between the received signal and the reference signal. The TOA measurements can be estimated by finding the peak of the cross correlation function, after which the receivers communicate these TOA measurements to calculate the TDOA measurements.

2.1 Time of Arrival Measurement

We choose GCC-PHAT to estimate the time delay between the transmitter and the receiver because GCC-PHAT is robust against multipath effects, which we will illustrate later in this chapter. Assume the transmitted signal, say $m(t)$, is uncorrelated with the noise and interferences at receiver j, say $n_j(t)$. The received signals at receivers are $g_1(t), \ldots, g_M(t)$. The attenuation of the signal received by sensor j is denoted by α_j, where $1 \leq j \leq M$. Moreover, let $g_0(t)$ denote the reference signal stored in each receiver. In addition, d_j is the time delay between the transmitter and the receiver j that we want to estimate.The signal received by receiver j can be modeled as

$$g_j(t) = \alpha_j m(t + d_j) + n_j(t),\ 1 \leq j \leq M, \tag{2.1}$$

where $m(t)$ and $n_j(t)$ are real jointly stationary random process.

2.1.1 Generalized Cross Correlation

A general method to estimate the time delay d_j is the generalized cross correlation (GCC). We will start from the cross correlation. The cross correlation between the received signal and the reference signal is

$$R_{g_0 g_j}(\tau) = E[g_0(t) g_j(t - \tau)], \tag{2.2}$$

where E denotes the expectation operator and τ denotes the time lags. The estimation of the time delay is provided by the argument τ that maximizes (2.2) [23], that is,

$$\hat{d_j} = \arg\max_{\tau} R_{g_0 g_j}(\tau). \tag{2.3}$$

The cross correlation function can also be computed through the inverse Fourier transform of the cross power spectral density function $P_{g_0 g_j}(f)$,

$$R_{g_0 g_j}(\tau) = \int_{-\infty}^{\infty} P_{g_0 g_j}(f) \mathrm{e}^{j2\pi f \tau} \, \mathrm{d}f. \tag{2.4}$$

Combine (2.1) with (2.2), under the assumption that the signals and noises are uncorrelated, we can derive

$$R_{g_0 g_j}(\tau) = \alpha_j R_{mm}(\tau - d_j) + R_{n_0 n_j}(\tau), \tag{2.5}$$

and the cross power spectral density is given by

$$P_{g_0 g_j}(f) = \alpha_j P_{mm}(f) \mathrm{e}^{-j2\pi f d_j} + P_{n_0 n_j}(f). \tag{2.6}$$

We assume the noise process is uncorrelated, we have $P_{n_0 n_j}(f) = 0$. With this, (2.5) can be reformulated as

$$R_{g_0 g_j}(\tau) = \alpha_j R_{mm}(\tau) * \delta(\tau - d_j), \tag{2.7}$$

where $*$ denotes the convolution operation. In addition, (2.6) can be expressed as

$$P_{g_0 g_j}(f) = \alpha_j P_{mm}(f) \mathrm{e}^{-j2\pi f d_j}. \tag{2.8}$$

According to (2.7), the delta function is spread by the auto-correlation function of the signal. For a single time delay estimation, spreading may not cause problems because $R_{g_0 g_j}(\tau)$ will peak at the time lag d_j whether it is spread out or not. However, in indoor localization, multipath effects may cause multiple delays of a single signal for one sensor. In this case, spreading can cause a serious problem. Let α_{ij} and d_{ij} denote the attenuation and the time delay at the receiver j from the ith path, respectively. In that case, we can express the cross correlation function as

$$R_{g_0 g_j}(\tau) = R_{mm}(\tau) * \sum_{i \in \mathcal{N}} \alpha_{ij} \delta(\tau - d_{ij}), \ 1 \leq j \leq M. \tag{2.9}$$

For multiple delays, the convolution may spread one delta function to another. As a consequence, it is difficult to distinguish peaks [23].

In order to improve the accuracy of the time delay estimation, we will pre-filter received signals before the correlation operation. Assume the signal g_j is filtered through the pre-filter H_j to yield y_j, where $0 \leq j \leq M$. The generalized cross correlation is provided through the introduction of the pre-filter for the estimation of the time delay d_j [23]. In order to distinguish with the ordinary cross correlation, we use the superscript $(.)^{(g)}$ and the subscript

g to represent the variables related to the generalized cross correlation. Consequently, the generalized cross correlation function is given by

$$R_{y_0y_j}^{(g)}(\tau) = \int_{-\infty}^{\infty} \psi_g(f) P_{g_0g_j}(f) \mathrm{e}^{j2\pi f\tau} \, \mathrm{d}f, \tag{2.10}$$

where $\psi_g(f) = H_0(f)H_j^*(f)$ is a general frequency weighting [23]. With this, the cross power spectral density of the filter output can be expressed as

$$P_{y_0y_j}(f) = H_0(f)H_j^*(f)P_{g_0g_j}(f), \tag{2.11}$$

where * represents complex conjugation [23].

However, in practice, since we do not know the statistics of the process, we can only get an estimation of the cross power spectral density, say $\hat{P}_{g_0g_j}(f)$, because of finite length of observations. With this, the generalized cross correlation function used for time delay estimation is

$$\hat{R}_{y_0y_j}^{(g)}(\tau) = \int_{-\infty}^{\infty} \psi_g(f) \hat{P}_{g_0g_j}(f) \mathrm{e}^{j2\pi f\tau} \, \mathrm{d}f. \tag{2.12}$$

With a proper weighting $\psi_g(f)$ and a proper estimation $\hat{P}_{g_0g_j}(f)$, the estimation of the time delay $\hat{d}_j = \arg\max_\tau \hat{R}_{g_0g_j}^{(g)}(\tau)$ can be obtained [23].

2.1.2 The Phase Transformation

One of the principles to choose the weighting function $\psi_g(f)$ is to ensure a large and sharp peak for a high time-delay resolution. However, a large and sharp peak is more sensitive to the errors which are introduced by finite length of observations, particularly when the signal to noise ratio (SNR) is relatively low. Hence, the choice of the weighting function is a compromise between the resolution and the stability [23].

The phase transformation proves to avoid the spreading out by the auto-correlation function of the signal, which is expressed as

$$\psi_g^{PHAT}(f) = \frac{1}{|P_{g_0g_j}(f)|}, \tag{2.13}$$

where we use the superscript $(.)^{PHAT}$ to denote the generalized cross correlation with phase transfrom. With this, (2.12) is expressed as

$$R_{y_0y_j}^{PHAT}(\tau) = \int_{-\infty}^{\infty} \frac{\hat{P}_{g_0g_j}(f)}{|P_{g_0g_j}(f)|} \mathrm{e}^{j2\pi f\tau} \, \mathrm{d}f. \tag{2.14}$$

According to (2.8), $|P_{g_0g_j}(f)| = \alpha_j P_{mm}(f)$. Under ideal conditions where the estimated cross power spectral density equals to the cross power spectral density, i.e., $\hat{P}_{g_0g_j}(f) =$

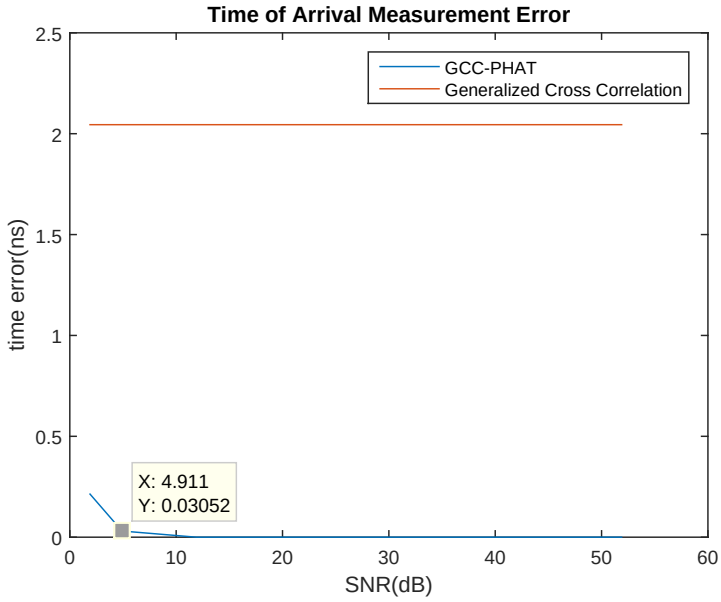

Figure 2.1: Time of Arrival Measurement Error

$P_{g_0g_j}(f)$, $\frac{\hat{P}_{g_0g_j}(f)}{|P_{g_0g_j}(f)|} = \mathrm{e}^{j\theta(f)} = \mathrm{e}^{j2\pi f d_j}$ has a unit magnitude. Accordingly, (2.14) can be expressed as [23]

$$R_{y_0y_j}^{PHAT}(\tau) = \delta(\tau - d_j). \tag{2.15}$$

In this case, only the phase information is preserved. Comparing with (2.7), (2.15) illustrates that under ideal conditions, there is no spreading when we use GCC-PHAT to estimate the time delay. As a consequence, it is suited to indoor environments with many reverberations. Since the cross correlation after the phase transformation is a delta function, the accuracy depends on the sampling frequency.

However, there are two disadvantages. The first one is that the generalized cross correlation function will not be a delta function if the estimated cross power spectral density is different from the cross power spectral density. Another disadvantage is since the weighting function is an inverse of the cross power spectral density, errors will be accentuated where signal power is relatively small. Especially, when the cross power spectral density is zero, the estimation will be erratic [23].

We will do a simulation to compare the error of the time of arrival measurements between the cross correlation method and GCC-PHAT. Figure 2.1 illustrates the simulation result.

As shown in the simulation result, GCC-PHAT always performs better than the cross correlation method. In fact, the cross correlation method is the generalized cross correlation method with all-pass filters. When the signal to noise ratio is no less than 5dB, the error of the time of arrival measurement with GCC-PHAT is no larger than 0.03ns. This is consistent with the previous explanation. When we use GCC-PHAT to estimate the time of arrival, we

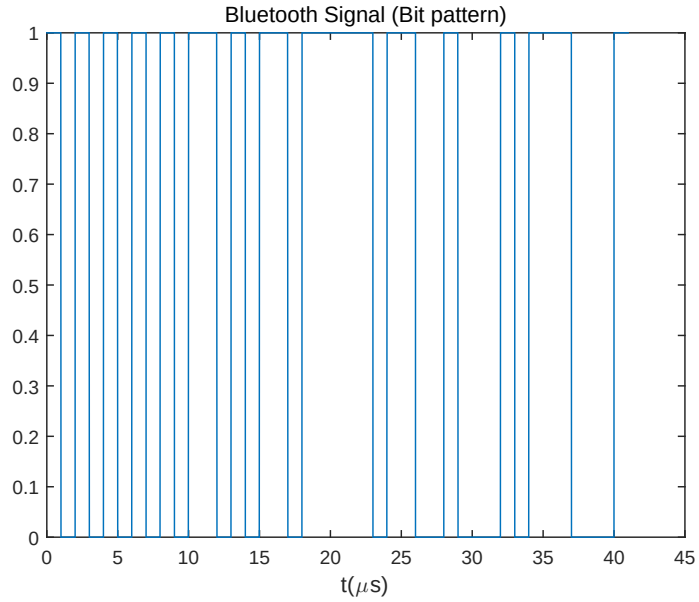

Figure 2.2: The Bit Pattern of the Bluetooth Signal

can achieve sampling accuracy. In our experiments, the sampling frequency is 32.8GHz. That is, the error of the time of arrival measurement is about 0.03ns. Because GCC-PHAT is relatively sensitive to noise, the error of the time of arrival measurement is large when the SNR is relatively low.

2.2 Signals for TOA measurements

In this section, we want to explore the signals that we use to explore the time of arrival information. Bluetooth signals can be divided into two signal segments. The first part is identical among all users. The second part is different, which is used to identify the different transmitters. In the thesis, the first part of Bluetooth signals is chosen for the TOA measurements because it is fixed. The bit pattern of the first part of Bluetooth signals is shown in Figure 2.2. In the thesis, GFSK modulation is chosen to avoid the large bandwidth faced by FSK. Under GFSK modulation, a Gaussian pre-modulation filter is applied first. After that, the output is used as the input of a voltage controlled oscillator (VCO), which converts the amplitude to a frequency shift [24]. The GFSK signal and the filtered baseband signal are shown in Figure 2.3.

There are two options for the signal used for TOA measurements, baseband Bluetooth signals and GFSK modulated Bluetooth signals. On the basis of GCC-PHAT, the accuracy depends on the sampling frequency. For the same sampling frequency, GFSK modulated signals can achieve the same accuracy as baseband signals. However, demodulation will introduce some distortion, which may result in incorrect TOA measurements. Considering the complexity and the accuracy, we decided to use GFSK modulated Bluetooth signals for

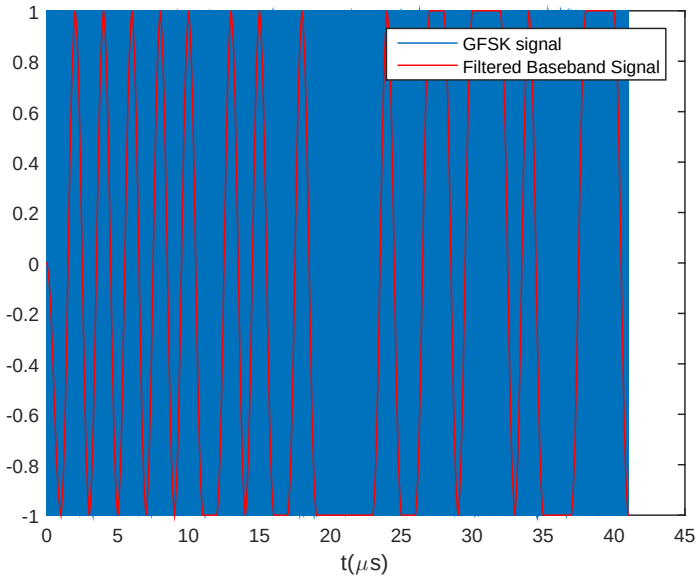

Figure 2.3: GFSK modulated Bluetooth Signal

TOA measurements in this thesis.

3 TDOA Localization

Since we already have TDOA measurements, we can do the localization. In this chapter, we would like to develop a centralized method for TDOA based localization and further, implement it in a distribute way. Moreover, we want to know the accuracy we can achieve with the proposed methods and compare it with the highest accuracy we may achieve, i.e., the Cramer-Rao lower bound. Based on the CRLB, we will examine the optimal way to place receivers.

3.1 Preliminary

Consider the situation with M receivers with known locations and one transmitter whose location is to be estimated with TDOA based techniques. Let $s_1, s_2, \ldots, s_M$ denote the location of receivers and s_0 denote the location of the transmitter. In a three dimensional space, the coordinate of the receivers and the transmitter can be represented by $s_j = (x_j, y_j, z_j)$ and $s_0 = (x_0, y_0, z_0)$, respectively. For receiver j, the time of arrival information is given by $\tau_j = c^{-1}|s_0 - s_j| + n_j$, where c is the speed of light, and n_j is the measurement noise at receiver j with $\mathrm{E}[N_j] = 0$ and $\mathrm{Var}[N_j] = \sigma_j^2 < \infty$. Moreover, we assume measurements are uncorrelated at different receivers. Without loss of generality, we choose receiver 1 as the reference receiver and assume receiver 1 is at the original point, i.e., $s_1 = (0, 0, 0)$.

3.2 Centralized Localization

Considering centralized localization, all TOA measurements are transmitted to a central computer. In this case, we choose the receiver 1 as the reference receiver to compute all TDOAs. Let $\Delta\tau_{1j}$ denote the TDOA measurement at receiver j, which is given by

$$\Delta\tau_{1j} = \tau_1 - \tau_j = c^{-1}|s_0 - s_1| - c^{-1}|s_0 - s_j| + n_{1j},\ 2 \leq j \leq M, \tag{3.1}$$

where n_{1j} is a Gaussian distributed measurement noise of TDOA measurement between receiver 1 and receiver j, $n_{1j} \sim \mathcal{N}(0, \sigma_{1j}^2)$. Because of uncorrelated measurements, $\sigma_{1j}^2 = \sigma_1^2 + \sigma_j^2$. The noiseless TDOA measurement at receiver j is defined as $h_{1j}(r) = c^{-1}|s_0 - s_1| - c^{-1}|s_0 - s_j|$.

The distance difference between receiver j and receiver 1, say r_{j1}, can be calculated from the time difference of arrival by multiplying it with the propagation speed of the signal, which is

$$r_{j1} = r_j - r_1 = \Delta\tau_{1j} \times c, \tag{3.2}$$

where $r_j = \sqrt{(x_j - x_0)^2 + (y_j - y_0)^2 + (z_j - z_0)^2}$ denotes the distance between the transmitter and the receiver j, c denotes the speed of the signal. With that, we can derive the following equation,

$$(r_{j1}+r_1)^2 = r_j^2 = (x_j-x_0)^2+(y_j-y_0)^2+(z_j-z_0)^2 = K_j^2-2x_jx_0-2y_jy_0-2z_jz_0+r_1^2, \quad (3.3)$$

where we define $K_j^2 = x_j^2 + y_j^2 + z_j^2$. Rewrite (3.3), we arrive at

$$-x_jx_0 - y_jy_0 - z_jz_0 = r_{j1}r_1 + \frac{1}{2}(r_{j1}^2 - K_j^2). \quad (3.4)$$

Write (3.4) in the vector form with $2 \leq j \leq M$,

$$\boldsymbol{A}s_0 = r_1\boldsymbol{c} + \boldsymbol{d}, \quad (3.5)$$

where

$$\boldsymbol{A} = \begin{bmatrix} x_2 & y_2 & z_2 \\ \vdots & \vdots & \vdots \\ x_M & y_M & z_M \end{bmatrix}, s_0 = \begin{bmatrix} x_0 \\ y_0 \\ z_0 \end{bmatrix}, \boldsymbol{c} = \begin{bmatrix} -r_{21} \\ \vdots \\ -r_{M1} \end{bmatrix}, \boldsymbol{d} = \frac{1}{2}\begin{bmatrix} K_2^2 - r_{21}^2 \\ \vdots \\ K_M^2 - r_{M1}^2 \end{bmatrix}.$$

Since the measurements are noisy, we would like to find a location estimation to minimize the noise,

$$\min_{s_0} ||\boldsymbol{A}s_0 - (r_1\boldsymbol{c} + \boldsymbol{d})||_2^2. \quad (3.6)$$

The least-squares solution to problem (3.5) is given by

$$\hat{s}_0 = (\boldsymbol{A}^T\boldsymbol{A})^{-1}\boldsymbol{A}^T(r_1\boldsymbol{c} + \boldsymbol{d}). \quad (3.7)$$

Combining the solution with $r_1^2 = x_0^2 + y_0^2 + z_0^2$, the location of the transmitter can be estimated [25].

3.3 Centralized Localization with Arbitrary Reference Sensor

In this case, all TOA measurements are still transmitted to a central computer. Instead of choosing receiver 1 as the reference receiver, we choose arbitrary receivers as the reference receiver. Afterwards, we average among them. Assume the receiver k is chosen as the reference receiver, and the estimated source location is denoted as s_{0k}. With this, the problem can be formulated as

$$\min_{s_{0k}} ||\boldsymbol{A}_k s_{0k} - (r_k\boldsymbol{c}_k + \boldsymbol{d}_k)||_2^2, \quad (3.8)$$

where

$$\boldsymbol{A}_k = \begin{bmatrix} x_1 - x_k & y_1 - y_k & z_1 - z_k \\ \vdots & \vdots & \vdots \\ x_{k-1} - x_k & y_{k-1} - y_k & z_{k-1} - z_k \\ x_{k+1} - x_k & y_{k+1} - y_k & z_{k+1} - z_k \\ \vdots & \vdots & \vdots \\ x_M - x_k & y_M - y_k & z_M - z_k \end{bmatrix}, s_0 = \begin{bmatrix} x_{0k} \\ y_{0k} \\ z_{0k} \end{bmatrix},$$

$$\boldsymbol{c}_k = \begin{bmatrix} -r_{1k} \\ \vdots \\ -r_{k-1k} \\ -r_{k+1k} \\ \vdots \\ -r_{Mk} \end{bmatrix}, \boldsymbol{d}_k = \frac{1}{2} \begin{bmatrix} K_1^2 - K_k^2 - r_{1k}^2 \\ \vdots \\ K_{k-1}^2 - K_k^2 - r_{k-1k}^2 \\ K_{k+1}^2 - K_k^2 - r_{k+1k}^2 \\ \vdots \\ K_M^2 - K_k^2 - r_{Mk}^2 \end{bmatrix}.$$

The estimated source location is given by the least-squares solution to problem (3.8),

$$\hat{s}_{0k} = (\boldsymbol{A}_k^T \boldsymbol{A}_k)^{-1} \boldsymbol{A}_k^T (r_k \boldsymbol{c}_k + \boldsymbol{d}_k). \tag{3.9}$$

Given M estimations in total, which are computed by M different reference receivers, we average among them to calculate the estimation of the transmitter's location, which is given by

$$\hat{s}_0 = \frac{1}{M} \sum_{k=1}^{M} \hat{s}_{0k}. \tag{3.10}$$

3.4 Decentralized Localization with Full Information

We would like to decentralize the problem step by step. In this case, in contrast to the previous methods, we will estimate the location of the source locally at each receiver. Assume each receiver gets access to full time of arrival information. Based on the information from the neighbors, the receivers can update the local estimation. The receivers will communicate with each other to get a consensus of an estimated location iteratively. With this, our problem is expressed as

$$\min_{s_{0k}} \sum_{k=1}^{M} ||\boldsymbol{A}_k s_{0k} - (r_k \boldsymbol{c}_k + \boldsymbol{d}_k)||_2^2,$$

$$\text{subject to } s_{0k} = s_{0j}, \forall (k,j) \in E, \tag{3.11}$$

where

$$\boldsymbol{A}_k = \begin{bmatrix} x_1 - x_k & y_1 - y_k & z_1 - z_k \\ \vdots & \vdots & \vdots \\ x_{k-1} - x_k & y_{k-1} - y_k & z_{k-1} - z_k \\ x_{k+1} - x_k & y_{k+1} - y_k & z_{k+1} - z_k \\ \vdots & \vdots & \vdots \\ x_M - x_k & y_M - y_k & z_M - z_k \end{bmatrix}, s_0 = \begin{bmatrix} x_{0k} \\ y_{0k} \\ z_{0k} \end{bmatrix},$$

$$\boldsymbol{c}_k = \begin{bmatrix} -r_{1k} \\ \vdots \\ -r_{k-1k} \\ -r_{k+1k} \\ \vdots \\ -r_{Mk} \end{bmatrix}, \boldsymbol{d}_k = \frac{1}{2} \begin{bmatrix} K_1^2 - K_k^2 - r_{1k}^2 \\ \vdots \\ K_{k-1}^2 - K_k^2 - r_{k-1k}^2 \\ K_{k+1}^2 - K_k^2 - r_{k+1k}^2 \\ \vdots \\ K_M^2 - K_k^2 - r_{Mk}^2 \end{bmatrix}$$

As a consequence, we can rewrite the problem (3.11) as a quadratic problem,

$$\min_{s_{0k}} \sum_{k=1}^{M} s_{0k}^T P_k s_{0k} + 2Q_k s_{0k} + b_k,$$

$$\text{subject to } s_{0k} = s_{0j}, \forall (k,j) \in E, \tag{3.12}$$

where

$$P_k = \boldsymbol{A}_k^T \boldsymbol{A}_k, Q_k = -(r_k \boldsymbol{c}_k + \boldsymbol{d}_k)^T \boldsymbol{A}_k, b_k = (r_k \boldsymbol{c}_k + \boldsymbol{d}_k)^T (r_k \boldsymbol{c}_k + \boldsymbol{d}_k),$$

which we can solve with PDMM. The details of PDMM will be presented in Chapter 3.7.

3.5 Decentralized Localization with Neighboring Information

Considering decentralized localization, each receiver computes a local estimated transmitter's location with the time of arrival information from its neighboring nodes. The local estimated transmitter's location measured by receiver k is denoted by s_{0k}. Based on the information from the neighbors, the receivers can update the local estimation. The receivers will communicate with each other to get a consensus of an estimated location iteratively. Assume the neighboring nodes of receiver k are denoted by $k_1, ..., k_{M_k}$, where $M_k = |\mathcal{N}_k|$ and $\mathcal{N}_k$ is the set of the neighboring nodes of node k. We assume the degree of each receiver is not smaller than 2, i.e., $|\mathcal{N}_k| \geq 2$. In addition, each receiver itself is considered as the reference receiver for location estimation. With this, our problem is expressed as

$$\min_{s_{0k}} \sum_{k=1}^{M_k} ||\boldsymbol{A}_k s_{0k} - (r_k \boldsymbol{c}_k + \boldsymbol{d}_k)||_2^2,$$

$$\text{subject to } s_{0k} = s_{0j}, \forall (k,j) \in E, \tag{3.13}$$

where

$$\boldsymbol{A}_k = \begin{bmatrix} x_{k_1} - x_k & y_{k_1} - y_k & z_{k_1} - z_k \\ \vdots & \vdots & \vdots \\ x_{k_M} - x_k & y_{k_M} - y_k & z_{k_M} - z_k \end{bmatrix}, s_{0k} = \begin{bmatrix} x_{0k} \\ y_{0k} \\ z_{0k} \end{bmatrix}, \boldsymbol{c}_k = \begin{bmatrix} -r_{k_1 k} \\ \vdots \\ -r_{k_M k} \end{bmatrix}, \boldsymbol{d}_k = \frac{1}{2} \begin{bmatrix} K_{k1}^2 - K_k^2 - r_{k_1 k}^2 \\ \vdots \\ K_{kM}^2 - K_k^2 - r_{k_M k}^2 \end{bmatrix}.$$

As a consequence, we can rewrite the problem (3.13) as a quadratic problem,

$$\min_{s_{0k}} \sum_{k=1}^{M} s_{0k}^T P_k s_{0k} + 2Q_k s_{0k} + b_k,$$

$$\text{subject to } s_{0k} = s_{0j}, \forall (k,j) \in E, \tag{3.14}$$

where

$$P_k = \boldsymbol{A}_k^T \boldsymbol{A}_k, Q_k = -(r_k \boldsymbol{c}_k + \boldsymbol{d}_k)^T \boldsymbol{A}_k, b_k = (r_k \boldsymbol{c}_k + \boldsymbol{d}_k)^T (r_k \boldsymbol{c}_k + \boldsymbol{d}_k),$$

which we can solve with PDMM. The details of PDMM will be presented in Chapter 3.7.

It is shown in Appendix A that using neighboring TDOA measurement information instead of full TDOA measurement information will not decrease the accuracy.

3.6 Low Rank Reformulation

When we place all the receivers on the ceiling, the rank of the problem is lower. In this case, the problem should be reformulated. To begin with, we discard the z coordinate and solve the problem with the two-dimensional method to determine the x and y coordinates. With the time of arrival information and the range of the z coordinate, we can calculate the corresponding z coordinate. In this way, we can also get an accurate estimated location.

3.7 PDMM Implementation

Since Section 3.4 and Section 3.5 have the same form, PDMM implementation is same except that the notation is different.

Use a graph $G = (V, E)$ to define the network, where V denotes the set of nodes and E denotes the set of edges between nodes. The separable objective function can be written as $f(x) = \sum_{i \in V} f_i(x_i)$. Let A_{ij} and A_{ji} with $i, j \in V$ denote the linear constraint matrices. In addition, c_{ij} is the coefficient of the linear constraint. With this, the standard primal-dual method of multipliers (PDMM), a node based optimization algorithm, is described as

$$\text{minimize } \sum_{i \in V} f_i(x_i),$$

$$\text{subject to } A_{ij} x_i + A_{ji} x_j = c_{ij}, \text{ for all } (i,j) \in E. \tag{3.15}$$

Comparing our linear constraints shown in (3.12) and (3.14) with the standard PDMM, we can get

$$c_{kj} = 0,$$

$$A_{kj} = \begin{cases} I & \text{if } k < j \\ -I & \text{otherwise} \end{cases},$$

where I denotes an identity matrix. If we write $A_{kj} = l_{kj} I$, where

$$l_{kj} = \begin{cases} 1 & \text{if } k < j \\ -1 & \text{otherwise} \end{cases},$$

we obtain $l_{kj}^2 = 1$ and $l_{kj} l_{jk} = -1$ [26].

In order to solve the problem (3.12) and (3.14), we define $f_k(s_{0k}) = s_{0k}^T P_k s_{0k} + 2Q_k s_{0k} + b_k$. The Lagrangian function is given by

$$L_p(s_0, \nu) = \sum_{k \in V} f_k(s_{0k}) + \sum_{(k,j) \in E} \nu_{kj}^T (-A_{kj} s_{0k} - A_{jk} s_{0j}), \tag{3.16}$$

where ν_{kj} are edge variables. Given the primal Lagrangian, the dual problem is given by

$$\begin{aligned} g(\nu) &= \inf_{s_0} \sum_{k \in V} (f_k(s_{0k}) - \sum_{j \in \mathcal{N}_k} \nu_{kj}^T A_{kj} s_{0k}) \\ &= -\sup_{s_0} \sum_{k \in V} (\sum_{j \in \mathcal{N}_k} \nu_{kj}^T A_{kj} s_{0k}) - f_k(s_{0k})). \end{aligned} \tag{3.17}$$

Hence, the problem can be expressed as

$$\max \sum_{k \in V} -f_k^*(\sum_{j \in \mathcal{N}_k} A_{kj}^T \nu_{kj}), \tag{3.18}$$

where f_k^* denotes the conjugate function of f_k [26].

To decouple the node decencies, for each edge $(k, j) \in E$, we introduce two auxiliary node variables $\lambda_{k|j}$ and $\lambda_{j|k}$, one for each node k and j, respectively. The node variable $\lambda_{k|j}$ is owned and updated at node k and related to node j. Hence, M_k new variables are introduced at node k. With this, the dual problem can be reformulated as

$$\max \sum_{k \in V} -f_k^*(A_{kj}^T \lambda_{k|j}),$$

$$\text{subject to } \nu_{kj} = \lambda_{k|j} = \lambda_{j|k} \text{ for all } (k, j) \in E. \tag{3.19}$$

The associated dual Lagrangian problem is given by

$$L_d(\nu, \lambda, y) = \sum_{k \in V} (-f_k^*(\sum_{j \in \mathcal{N}_k} A_{kj}^T \lambda_{k|j}) + \sum_{j \in \mathcal{N}_k} y_{k|j}^T (\nu_{kj} - \lambda_{k|j})). \tag{3.20}$$

At a saddle point of L_d, we arrive at

$$0 \in \partial_{\lambda_{k|j}} L_d(\nu^*, \lambda^*, y^*) = \partial_{\lambda_{k|j}} f_k^*(\sum_{j \in \mathcal{N}_k} A_{kj}^T \lambda_{k|j}) + y_{k|j}^*. \tag{3.21}$$

On the other hand, Frenchel's inequality must hold with equality. In that case, we can derive

$$0 \in \partial_{\lambda_{k|j}} f_k^*(\sum_{j\in\mathcal{N}_k} A_{kj}^T \lambda_{k|j}) + A_{jk} s_{0j}^*. \tag{3.22}$$

Therefore, at a saddle point, we have $y_{k|j}^* = A_{jk} s_{0j}^*$. In this case, we restrict the Lagrange multipliers $y_{k|j}$ to be of the form $y_{k|j} = A_{jk} s_{0j}$. As a consequence, the dual Lagrangian problem is given by [26]

$$L_d(\nu, \lambda, s_0) = \sum_{k\in V}(-f_k^*(\sum_{j\in\mathcal{N}_k} A_{kj}^T \lambda_{k|j}) - \sum_{j\in\mathcal{N}_k} \lambda_{j|k}^T A_{kj} s_{0k} - \sum_{(k,j)\in E} \nu_{kj}^T(-A_{kj} s_{0k} - A_{jk} s_{0j}). \tag{3.23}$$

Define the primal-dual Lagrangian function

$$L_{pd}(s_0, \lambda) = L_p(s_0, \nu) + L_d(\nu, \lambda, s_0) = \sum_{k\in V}(f_k(s_{0k}) - f_k^*(\sum_{j\in\mathcal{N}_k} A_{kj}^T \lambda_{k|j}) - \sum_{j\in\mathcal{N}_k} \lambda_{j|k}^T A_{kj} s_{0k}), \tag{3.24}$$

which is convex in s_0 for fixed λ and concave in λ for fixed s_0 [26].

To enforce the primal feasibility, we introduce two penalty terms,

$$L_\rho(s_0, \lambda) = L_{pd}(s_0, \lambda) + h_p(s_0) - h_d(\lambda), \tag{3.25}$$

where

$$h_p(s_0) = \sum_{(k,j)\in E} \frac{\rho_p}{2} ||A_{kj} s_{0k} + A_{jk} s_{0j}||^2,$$

$$h_d(\lambda) = \sum_{(k,j)\in E} \frac{\rho_d}{2} ||\lambda_{k|j} - \lambda_{j|k}||^2.$$

Moreover, in order to simplify the equations and be able to use a broadcast protocol, we use $\rho = \rho_p = \rho_d^{-1}$ [26].

Solving the minimization problem, we can arrive at the update scheme,

$$\begin{aligned} s_{0k}^{(i+1)} &= arg\min_{s_{0k}}(f_k(s_{0k}) - s_{0k}^T(\sum_{j\in\mathcal{N}_k} A_{kj}^T \lambda_{j|k}^{(i)}) + \sum_{j\in\mathcal{N}_k} \frac{\rho_p}{2} ||A_{kj} s_{0k} + A_{jk} s_{0j}^{(i)}||^2) \\ &= (2P_k + \sum_{j\in\mathcal{N}_k} \rho)^{-1}(-2Q_k + \sum_{j\in\mathcal{N}_k}(l_{kj}\lambda_{j|k}^{(i)} + \rho s_{0j}^{(i)})), \end{aligned} \tag{3.26}$$

$$\begin{aligned} \lambda_{k|j}^{(i+1)} &= arg\min_{\lambda_k}(f_k^*(\sum_{j\in\mathcal{N}_k} A_{kj}^T \lambda_{k|j}) + \sum_{j\in\mathcal{N}_k} \lambda_{j|k}^T A_{kj} s_{0k}^{(i)} + \sum_{j\in\mathcal{N}_k} \frac{\rho_d}{2} ||\lambda_{k|j} - \lambda_{j|k}^{(i)}||^2) \\ &= \lambda_{j|k}^{(i)} - l_{kj}\rho(s_{0k}^{(i+1)} - s_{0j}^{(i)}),\ \forall (k,j) \in E, \end{aligned} \tag{3.27}$$

where $^{(i)}$ denotes the ith iteration.
The PDMM implementation is summarized in Algorithm 1. As a consequence, we have $\lim_{i\to\infty} s_{0k}^{(i)} = s_0$ for all $k \in V$

Algorithm 1 TDOA Localization with PDMM

At iteration $i+1$,

1. Select node k uniformly at random.
2. Update $s_{0k}^{(i+1)}$ by solving $0 \in \partial_{s_{0k}} L_\rho(s_0^{(i)}, \lambda^{(i)})$, which gives

$$s_{0k}^{(i+1)} = (2P_k + \sum_{j \in \mathcal{N}_k} \rho)^{-1}(-2Q_k + \sum_{j \in \mathcal{N}_k} (l_{kj}\lambda_{j|k}^{(i)} + \rho s_{0j}^{(i)}))$$

.

3. Broadcast $s_{0k}^{(i+1)}$ to neighboring nodes $j \in \mathcal{N}_k$.
4. Update $\lambda_{k|j}^{(i+1)} = \lambda_{j|k}^{(i)} - l_{kj}\rho(s_{0k}^{(i+1)} - s_{0j}^{(i)}),\ \forall j \in \mathcal{N}_k$

3.8 Cramer-Rao Lower Bound

In order to examine the highest accuracy we may achieve with TDOA localization, we would like to study the Cramer-Rao lower bound. In this case, we will calculate the variance of localization with a fixed reference receiver, i.e., the receiver 1. With the TDOA measurement defined in (3.1), the probability distribution function of the TDOA measurement can be derived as

$$p(\Delta\tau_{1j}|s_j) = \frac{1}{\sqrt{2\pi}\sigma_{1j}} exp(-\frac{1}{2\sigma_{1j}^2}(\Delta\tau_{1j} - h_{1j}(r))^2). \tag{3.28}$$

We can write TDOA measurements in the vector form

$$\boldsymbol{\Delta\tau} = \boldsymbol{h}(s_0) + \boldsymbol{n}, \tag{3.29}$$

where $\boldsymbol{\Delta\tau} = (\Delta\tau_{12}, \Delta\tau_{13}, \ldots, \Delta\tau_{1M}) \in \mathcal{R}^{M-1}$, $\boldsymbol{h}(s_0) = (h_{12}(s_0), h_{13}(s_0), \ldots, h_{1M}(s_0)) \in \mathcal{R}^{M-1}$, $\boldsymbol{n} = (n_{12}, n_{13}, \ldots, n_{1M}) \in \mathcal{R}^{M-1}$ and $\boldsymbol{n} \sim \mathcal{N}(0, \boldsymbol{R})$ with $\boldsymbol{R} = \begin{pmatrix} \sigma_1^2 + \sigma_2^2 & \sigma_1^2 & \cdots & \sigma_1^2 \\ \sigma_1^2 & \sigma_1^2 + \sigma_3^2 & \cdots & \sigma_1^2 \\ \vdots & \vdots & \ddots & \vdots \\ \sigma_1^2 & \sigma_1^2 & \cdots & \sigma_1^2 + \sigma_M^2 \end{pmatrix}$

The likelihood function can be formulated as

$$p(\boldsymbol{\Delta\tau}|\mathbf{s}) = \frac{1}{(2\pi)^{\frac{M-1}{2}}\sqrt{|\boldsymbol{R}|}} exp(-\frac{1}{2}(\boldsymbol{\Delta\tau} - \boldsymbol{h}(s_0))^T)\boldsymbol{R}^{-1}(\boldsymbol{\Delta\tau} - \boldsymbol{h}(s_0)). \tag{3.30}$$

The Cramer-Rao lower bound is the inverse of Fisher information matrix, which is given by

$$FIM = E[\bigtriangledown_{s_0} lnp(\boldsymbol{\Delta\tau}|\boldsymbol{s})(\bigtriangledown_{s_0} lnp(\boldsymbol{\Delta\tau}|\boldsymbol{s}))^T]. \tag{3.31}$$

Insert the likelihood function (3.30), we arrive at

$$FIM = (\frac{\partial \boldsymbol{h}(s_0)}{\partial s_0})^T \boldsymbol{R}^{-1} \frac{\partial \boldsymbol{h}(s_0)}{\partial s_0}, \tag{3.32}$$

where $\frac{\partial \boldsymbol{h}(s_0)}{\partial s_0} = [\frac{\partial h_{12}(s_0)}{\partial s_0}, \ldots, \frac{\partial h_{1M}(s_0)}{\partial s_0}]^T$, and $\frac{\partial h_{1j}(s_0)}{\partial s_0} = c^{-1} \times (\frac{x_0-x_1}{|s_0-s_1|} - \frac{x_0-x_j}{|s_0-s_j|}, \frac{y_0-y_1}{|s_0-s_1|} - \frac{y_0-y_j}{|s_0-s_j|}, \frac{z_0-z_1}{|s_0-s_1|} - \frac{z_0-z_j}{|s_0-s_j|})$

With this, we can obtain the CRLB for the variance of TDOA based localization,

$$var(\hat{s_0}) \geq tr(FIM^{-1}) \tag{3.33}$$

There are three conclusions which can be derived from the CRLB. Firstly, only when $M \geq 3$, the existence of the CRLB can be guaranteed. Moreover, no minimum variance unbiased (MVU) estimators can achieve the CRLB under the Gaussian error model. It can be proved with the PDF, the derivative of PDF with respect to s_0 is given by

$$\bigtriangledown_{s_0} lnp(\boldsymbol{\Delta\tau}|\boldsymbol{s}) = (\frac{\partial \boldsymbol{h}(s_0)}{\partial s_0})^T \boldsymbol{R}^{-1}(\boldsymbol{\Delta\tau} - \boldsymbol{h}(s_0)). \tag{3.34}$$

If there exist an MVU estimator, the bound must be attained by all $\boldsymbol{\Delta\tau}$. That is, the derivative of PDF should be of the form

$$\bigtriangledown_{s_0} lnp(\boldsymbol{\Delta\tau}|\boldsymbol{s}) = I(\boldsymbol{s})(g(\boldsymbol{\Delta\tau}) - \boldsymbol{s}), \tag{3.35}$$

for some functions g and I, where $g(\boldsymbol{\Delta\tau})$ is an MVU estimator. Comparing (3.34) and (3.35), it can be concluded that they can not be same. As a consequence, an MVU estimator can not exist under the Gaussian error model. Last, we would like to examine which variables will have an influence on the CRLB. According to (3.32), the CRLB can be affected by TOA measurement variances. Since the norm of $(\frac{x_0-x_j}{|s_0-s_j|}, \frac{y_0-y_j}{|s_0-s_j|}, \frac{z_0-z_j}{|s_0-s_j|})$ equals to 1, the relative direction, instead of the distance between the transmitters and the receivers, have an influence on the CRLB. In other words, the distribution of the sensors will affect the CRLB [27].

3.9 Optimal Sensor Geometry

For simplicity, we examine the best way to place receivers in a two-dimensional plane. The optimal sensor geometry can be derived by minimizing the CRLB.

Rewrite $\frac{\partial h_{1j}(s_0)}{\partial s_0} = c^{-1} \times [(\frac{x_0-x_1}{|s_0-s_1|}, \frac{y_0-y_1}{|s_0-s_1|}) - (\frac{x_0-x_j}{|s_0-s_j|}, \frac{y_0-y_j}{|s_0-s_j|})]$ at first. Given the unit norm, $(\frac{x_0-x_j}{|s_0-s_j|}, \frac{y_0-y_j}{|s_0-s_j|}) = (\cos(\theta_j), \sin(\theta_j))$, where θ_j is the incline angle from the transmitter to the jth receiver [28].

We assume variances are equal among receivers, the covariance matrix can be written as $\mathbf{R} = \sigma^2(\mathbf{I}_{M-1} + \mathbf{1}_{M-1}\mathbf{1}_{M-1}^T)$, where $\mathbf{I}_{M-1}$ denotes the $(M-1) \times (M-1)$ identity matrix and $\mathbf{1}_{M-1}$ denotes $(M-1) \times 1$ all one vector. Hence, we can derive the inverse of the covariance matrix,

$$\boldsymbol{R}^{-1} = \frac{1}{M\sigma^2}(M\boldsymbol{I}_{M-1} - \mathbf{1}_{M-1}\mathbf{1}_{M-1}^T). \tag{3.36}$$

Combine (3.36) with

$$\frac{\partial \boldsymbol{h}(s_0)}{\partial s_0} = \begin{bmatrix} \cos\theta_2 - \cos\theta_1 & \sin\theta_2 - \sin\theta_1 \\ \vdots & \vdots \\ \cos\theta_M - \cos\theta_1 & \sin\theta_M - \sin\theta_1 \end{bmatrix},$$

the Fisher information matrix is given by

$$FIM = (\frac{\partial \mathbf{h}(s_0)}{\partial s_0})^T \mathbf{R}^{-1} \frac{\partial \mathbf{h}(s_0)}{\partial s_0} = \frac{1}{Mc^2\sigma^2} \times$$

$$\begin{bmatrix} (M-1)\sum_{k=1}^{M}\cos^2(\theta_k) - \sum_{i\neq j}^{M}\cos(\theta_i)\cos(\theta_j) & M\sum_{k=1}^{M}\cos(\theta_k)\sin(\theta_k) - \sum_{k=1}^{M}\cos(\theta_k)\sum_{k=1}^{M}\sin(\theta_k) \\ M\sum_{k=1}^{M}\cos(\theta_k)\sin(\theta_k) - \sum_{k=1}^{M}\cos(\theta_k)\sum_{k=1}^{M}\sin(\theta_k) & (M-1)\sum_{k=1}^{M}\sin^2(\theta_k) - \sum_{i\neq j}^{M}\sin(\theta_i)\sin(\theta_j) \end{bmatrix}. \tag{3.37}$$

With this, the CRLB can be expressed as $f(\Theta)$, where $\Theta = [\theta_1, \theta_2, \ldots, \theta_M]$ [28],

$$var(\hat{s_0}) \geq tr(FIM^{-1}) = f(\boldsymbol{\Theta})$$

$$= \frac{M(M-1) - 2\sum_{i>j}^{M}\cos(\theta_i - \theta_j)}{M(M-2)\sum_{i>j}^{M}\sin^2(\theta_i - \theta_j) + 2M\sum_{k=1}^{M}\sum_{i>j}^{M}\sin(\theta_k - \theta_j)\sin(\theta_i - \theta_k)}. \tag{3.38}$$

(3.38) illustrates that the CRLB does not depend on the choice of the reference receiver.

To find the optimal sensor geometry, the derivative of $f(\Theta)$ with respect to θ_k, $k = 1, \ldots, M$ should equal to zero. Use $u(\Theta) > 0$ and $v(\Theta) > 0$ as the numerator and denominator, respectively, we arrive at

$$\left.\frac{\partial u(\Theta)}{\partial \theta_k}\right|_{\theta_k=\hat{\theta}_k} = f(\Theta) \left.\frac{\partial v(\Theta)}{\partial \theta_k}\right|_{\theta_k=\hat{\theta}_k}, k = 1, \ldots, M, \tag{3.39}$$

where $[\hat{\theta}_1, \ldots, \hat{\theta}_M]$ denotes the optimal incline angle from the transmitter to the receivers. (3.39) can be further simplified to

$$\left.\frac{\partial u(\Theta)}{\partial \theta_k}\right|_{\theta_k=\hat{\theta}_k} = 0 \text{ and } \left.\frac{\partial v(\Theta)}{\partial \theta_k}\right|_{\theta_k=\hat{\theta}_k}, k = 1, \ldots, M. \tag{3.40}$$

The equation (3.40) can only be satisfied if

$$\sum_{k=1}^{M}\cos(\hat{\theta}_k) = 0, \sum_{k=1}^{M}\sin(\hat{\theta}_k) = 0, \sum_{k=1}^{M}\cos(2\hat{\theta}_k) = 0, \sum_{k=1}^{M}\sin(2\hat{\theta}_k) = 0. \tag{3.41}$$

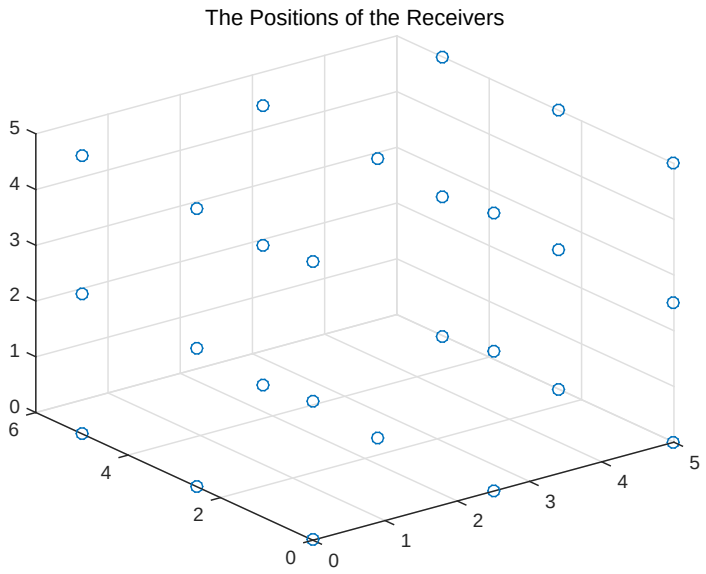

Figure 3.1: Receiver Distribution

A set of solution to (3.41) is given by

$$\hat{\theta}_k = \frac{2\pi}{M}(k-1) + \phi, \quad k = 1, \ldots, M, \tag{3.42}$$

where $\phi \in (0, 2\pi)$, which corresponds to a uniform angular array (UAA) [28].

However, in real applications, the transmitter's location cannot be known a prior. So the model with the transmitter uncertainty is important to study [29].

3.10 Numerical Simulation

In this section, we present some experimental results by computer simulation.

In the first simulation, we would like to compare the accuracy of four localization methods. We compare the estimated source location with the real source location to calculate the variance and compare the variance of localization with the Cramer-Rao lower bound. Assume the room is 5m$\times$5m$\times$5m with 26 receivers uniformly distributed on the boundaries. The positions of the receivers are shown in Figure 3.1. The transmitter's position is randomly deployed according to a uniform distribution. We perform 100 random configurations. In each configuration, the TOA measurement variance is deployed according to a Gaussian distribution. In order to compute the variance of the localization, we average the variances among 100 configurations. The simulation result in shown in Figure 3.2.

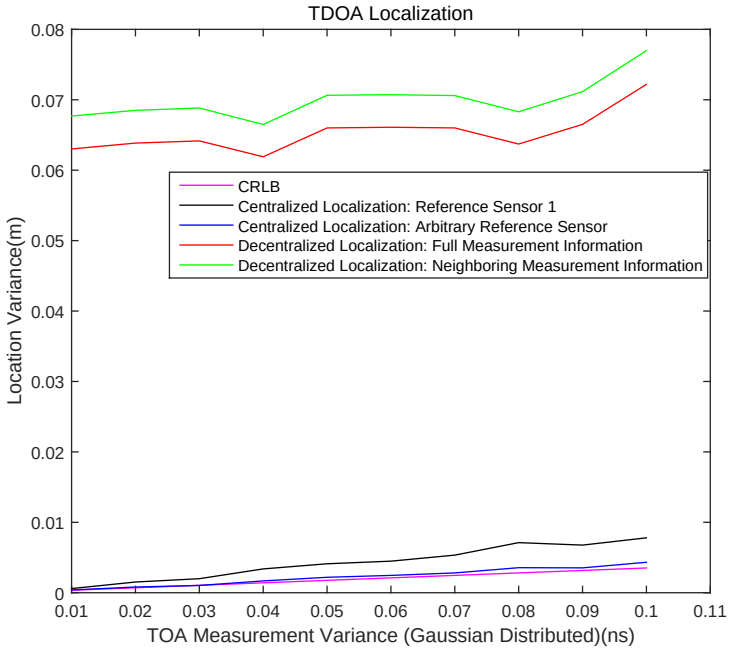

Figure 3.2: TDOA Localization with Gaussian Measurement Error

The simulation result shows that the four proposed methods perform well and the variance of the localization is close to the CRLB. As what is shown in Chapter 2, the time of arrival measurement variance is no larger than 0.03ns when the SNR is no less than 5dB. According to Figure 3.2, when the time of arrival variance is 0.03ns, the variance of the localization is within one centimeter. We can arrive at the conclusion, the four time difference of arrival localization methods are relatively accurate. The centralized localization with the arbitrary reference receiver performs a little bit better than the centralized localization with one fixed reference receiver because more TOA information is used for location estimation.

In the second simulation, we would like to examine the effect of the different measurement error distribution. In Figure 3.3, the TOA measurement error is uniformly distributed. Comparing with the simulation result shown in Figure 3.2, there is not much difference between two error distribution. It is reasonable because the uniformly distributed noise can be transformed into the Gaussian distributed noise.

In the following simulations, for simplicity and a better view of the receivers' distribution, we will do the simulations in a two-dimensional plane.

In the third simulation, we would like to examine the effect of the choice of the reference sensor on the variance of the localization in the difference receiver geometries. In a 20m$\times$20m room, we have four receivers and one transmitter. Firstly, we fix the transmitter in the room center. The receiver positions are randomly deployed according to a uniform distribution. We perform 500 random configurations. In each configuration, the variance of

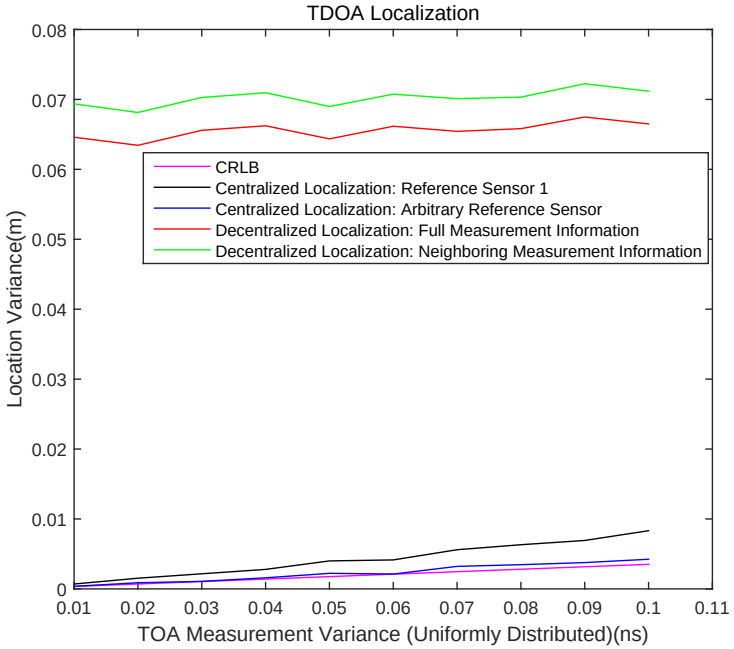

Figure 3.3: TDOA Localization with Uniformly Distributed Measurement Error

the TOA measurement is deployed according to a Gaussian distribution. In order to compute the variance of the localization, we average the variances among 500 configurations. In the second receiver geometry, instead of random receivers' positions, the four receivers are placed at the corners of a two-dimensional plane, which can be considered as a UAA. The simulation results are shown in Figure 3.4 and Figure 3.5.

Comparing these two receiver geometries, we can arrive at four conclusions. Firstly, the averaging method always performs better than choosing a specific reference sensor. Secondly, the choice of the reference receiver for the centralized algorithm is important, which will have an effect on the accuracy. When the receivers are uniformly angular distributed, it does not matter which receiver is chosen to be the reference sensor. However, when the receivers are randomly distributed, it is always better to choose the reference receiver whose incline angle is close to a uniform distribution, for example, the distribution of receivers 1, 2, 3 in Figure 3.4 is close to a UAA and they perform relatively better than receiver 4.

From the third simulation, we already know the choice of reference sensor will result in different localization accuracy in some receiver geometries. We would like to examine the best way to place all receivers. Because the CRLB is a theoretical lower bound of the variance of the localization, it can be used as an indicator in our simulation. Before the simulation, we have to make sure whether the CRLB will be affected by the choice of reference receiver. The simulation result is shown in Figure 3.6.

As what is shown in Figure 3.6, the choice of the reference receiver does not affect the

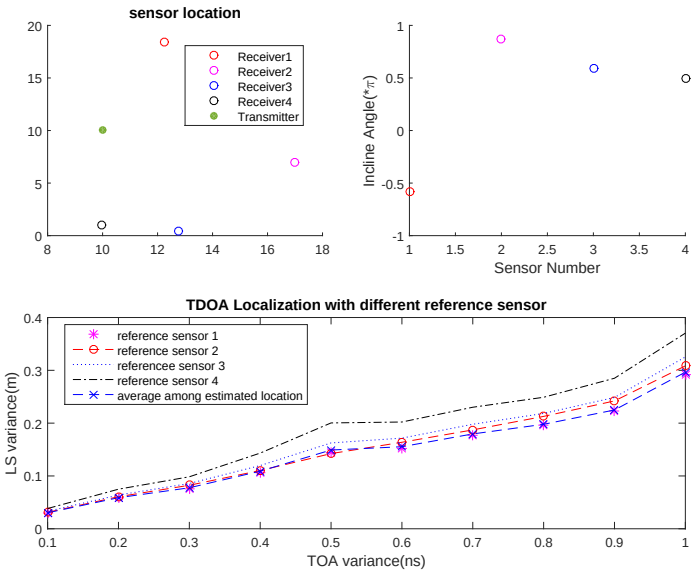

Figure 3.4: TDOA Localization1

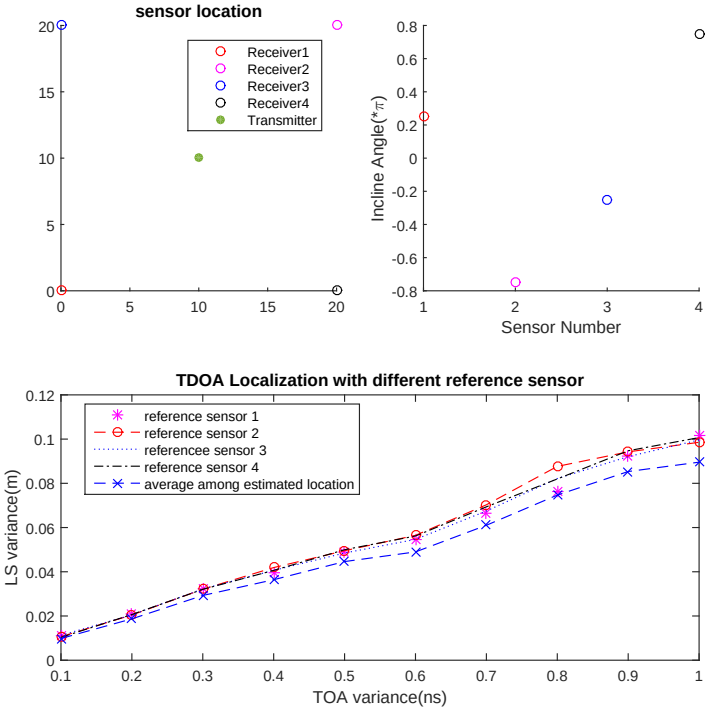

Figure 3.5: TDOA Localization2

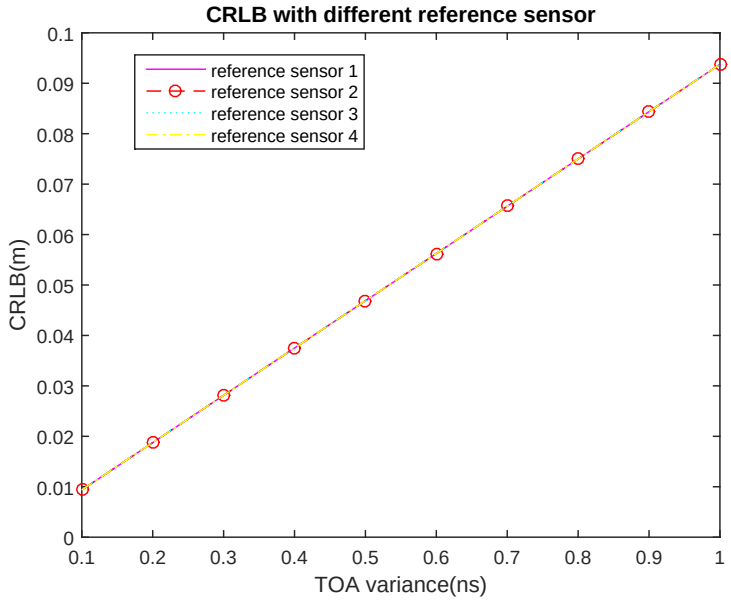

Figure 3.6: CRLB of TDOA Localization with different reference sensor

CRLB. As a result, it does not matter which reference sensor to choose when we use the CRLB to determine the receiver geometry.

In the fourth simulation, we would examine the optimal sensor geometry. We first generate a transmitter position, which is uniformly distributed on the plane. We compare the Cramer-Rao lower bound between the uniformly angular distributed receivers and the randomly distributed receivers. The simulation result is shown in Figure 3.7.

Based on the experimental result, we can conclude that lower CRLB can be attained when the receiver geometry is a UAA. Consequently, the receivers should be placed according to the uniform angular array in the room.

In the fifth simulation, we will examine the effect of the range of the receivers. Firstly, we fix the transmitter in the center. The first geometry is that the receivers are at the corners of a 20m$\times$20m plane. The second geometry is that the receivers are at the corners of the centering 12m$\times$12m plane. That is, the incline angle is uniformly distributed and the only difference is the range. Secondly, we want to know whether the transmitter should be inside the range of the receivers. The receivers are placed at four corners on the 20m$\times$20m plane and the left-bottom 10m$\times$10m plane, respectively. The transmitter is placed on the right-up 10m$\times$10m plane randomly. Compare the CRLB between two geometries. The simulation results are shown in Figure 3.8 and Figure 3.9.

The simulation result shows when the transmitter is in the range of the receivers, it does not matter what the range of the receivers is. However, when the transmitter is outside the range of receivers, the localization accuracy decreases significantly. As a consequence, we should

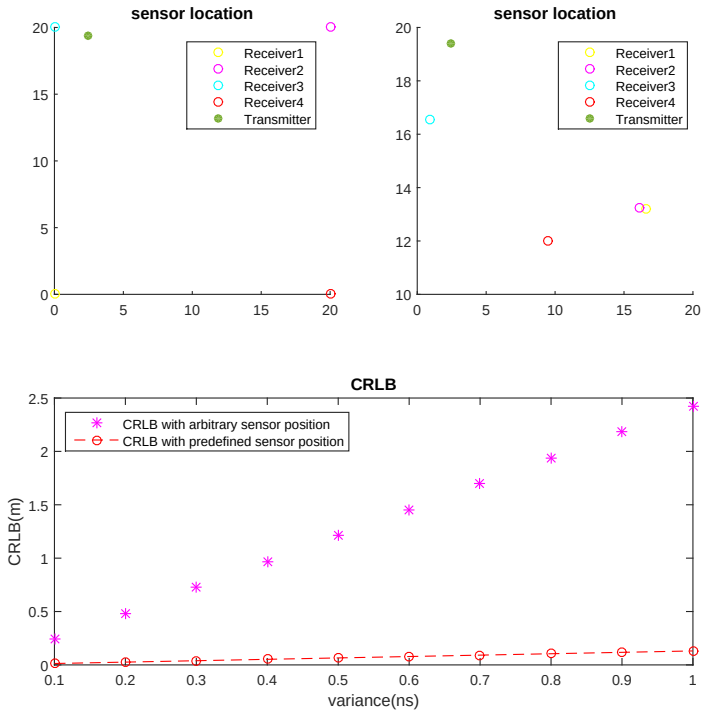

Figure 3.7: CRLB of TDOA Localization with different sensor geometry

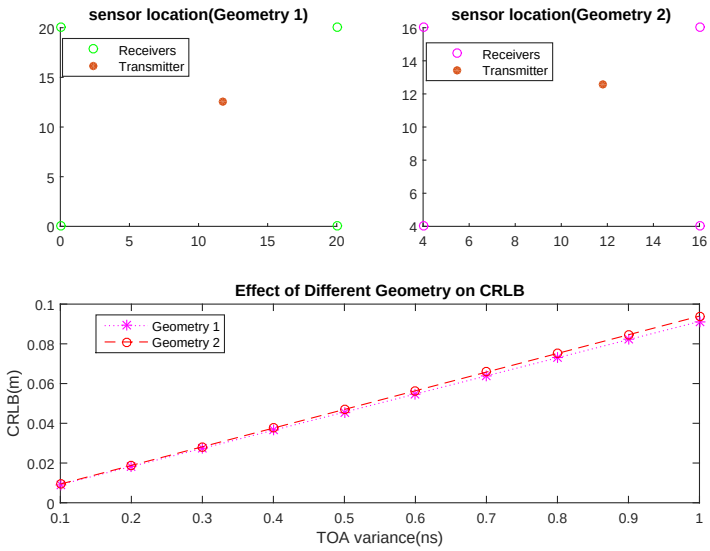

Figure 3.8: CRLB of TDOA Localization with different sensor sensor range

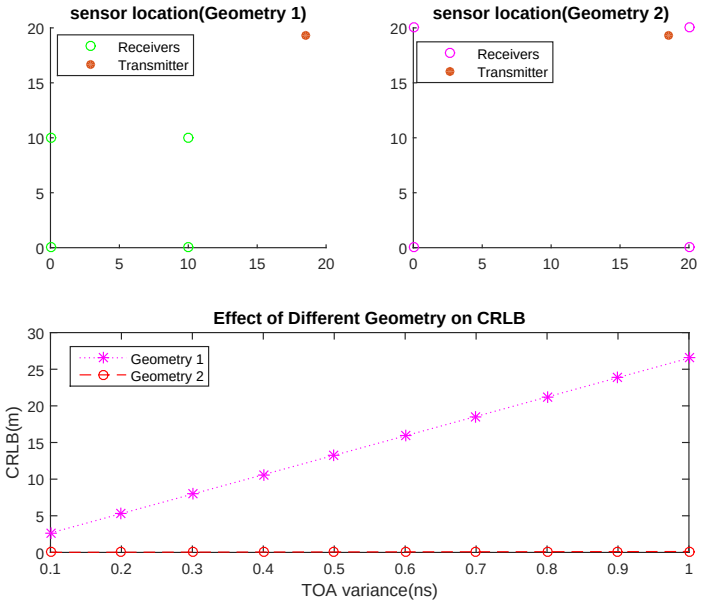

Figure 3.9: CRLB of TDOA Localization with different sensor geometry(Whether inside the range of Receivers)

place the receivers on the boundaries to make sure the transmitter will always be inside the range of the receivers.

We have already known that we should place the receivers on the boundaries, but we still don't know whether we should place all the receivers on the boundary or we only need to guarantee there are some receivers on the boundary. The first receiver geometry is that all 8 receivers are on the boundaries and they are uniformly distributed. The second receiver geometry is that only 4 receivers are at the corners of the plane and the other 4 receivers are randomly placed on the plane. The transmitter is randomly placed on the plane. In the sixth simulation, we will compare the accuracy between these two receivers geometries. The simulation result is shown in Figure 3.10.

To conclude, we should place all the sensors uniformly on the boundaries.

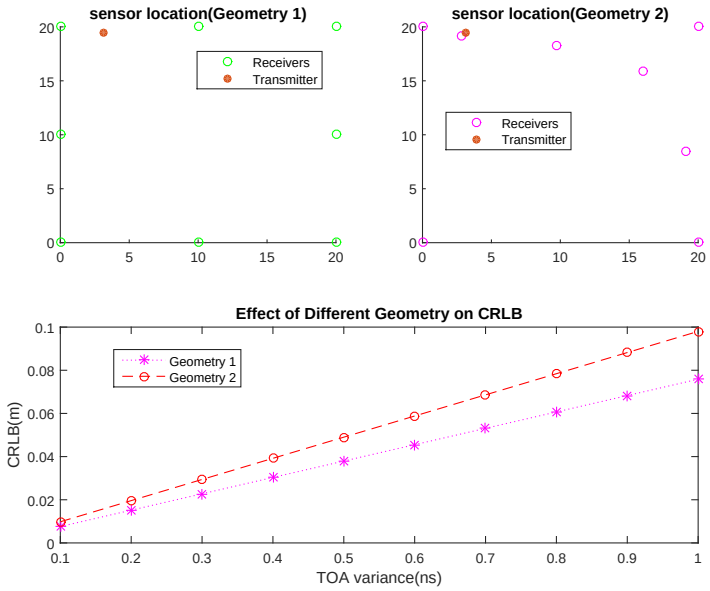

Figure 3.10: CRLB of TDOA Localization with different sensor geometry(Whether all on the boundaries)

4 Practical Aspects

In Chapter 2 and Chapter 3, we have already known how to measure TDOAs and use the measurements for localization. However, when they are used in real world applications, there are still some practical problems that we need to solve. We need to know how many sources we can accurately localize simultaneously one indoor environment. How to deal with multipath effects? Moreover, what if the line-of-sight is blocked in indoor environments? Last but not least, we want to know how to get the correct estimated location if there are some errors when we transmit the time of arrival information. All the questions will be answered in this chapter.

4.1 Multiple Users

For one Bluetooth transmitter, the time interval between two transmissions is assumed to be uniformly distributed in $25 \pm 5ms$. The length of the advertisement signal is variable, but the maximum length is $376\mu s$. The transmission is assumed to be independent of each other. We want to calculate the probability that no transmitters transmit Bluetooth signals at the same time. If there are no overlapped transmitted signal, we can localize the source accurately.

To begin with, divide the time $[0, \infty)$ into sufficiently small sub-intervals. The length of one interval is assumed to be Δ. Use $N(t)$ to denote the number of transmissions at time t. Assume the transmission rate is λ transmissions per unit time [30]. Since the time interval between two transmissions is assumed to be uniformly distributed in $25 \pm 5ms$, $\lambda = 1/25ms$.

A set of binary random variables are defined as

$$Y_m = \begin{cases} 1 & \text{if transmission is in the interval } (m\Delta, (m+1)\Delta] \\ 0 & \text{otherwise} \end{cases} . \tag{4.1}$$

Therefore,

$$EY_m = Pr\{Y_m = 1\} = \lambda\Delta = p. \tag{4.2}$$

To conclude, $N(t) \sim$ Bionomial (n, p), where $n \approx t/\Delta$ [30].

As $\Delta \to 0$, the probability mass function of $N(t)$ converges to a rate λt Poisson distribution, i.e., the number of transmissions in the time interval of length T follows a rate λT Poisson distribution. It can be expressed as

$$p_N(\lambda T, n) = \frac{(\lambda T)^n}{n!} e^{-\lambda T}, \quad n = 0, 1, 2, \ldots . \tag{4.3}$$

Note that the intervals between two transmissions at each transmitter, $X_1, X_2, \ldots$, are independent identically distributed sequences with an exponential distribution,

$$Pr\{X_n > x\} = Pr\{N(x) = 0\} = e^{-\lambda x}. \tag{4.4}$$

Hence, we have [30]

$$F_{X_n}(x) = Pr\{X_n \leq x\} = 1 - e^{-\lambda x}, \tag{4.5}$$

and

$$f_X(x) = f_{X_n}(x) = \frac{dF_{X_n}(x)}{dx} = \lambda e^{-\lambda x}. \tag{4.6}$$

Since the intervals between two transmissions at each transmitter are exponentially distributed with rate λ and independent across all transmitters and over time, the problem of n transmitters is equivalent to the problem that a single transmitter transmits Bluetooth signals according to a rate $n\lambda$ Poisson process at times Z_k and the interval $\{Z_{k+1} - Z_k\}$ are independent identically distributed sequences with an exponential distribution. Use q_k to denote the interval $\{Z_{k+1} - Z_k\}$, we have [30]

$$F(q) = 1 - e^{-n\lambda q}, \tag{4.7}$$

and

$$f(q) = \lambda e^{-n\lambda q}. \tag{4.8}$$

Given that the maximum length of the advertisement signal is $376\mu s$, the probability that there are no overlapped transmissions can be considered as the probability that the time interval between two transmissions should be larger than $376\mu s$. In this case, the probability is given by

$$Pr\{\text{No two transmitters will transmit at the same time}\} = 1 - F(376\mu s). \tag{4.9}$$

At the end of this section, we would like to examine the relationship between the probability of no overlapped transmitted signal and the number of transmitters. Moreover, we would like to examine the effect of the changed time interval between two transmissions. The simulation result is shown in Figure 4.1.

The simulation result shows when there are ten transmitters in the room, the probability that no transmitter transmits signals at the same time is about 86%. As the average time interval between two transmissions increases, the probability of no overlapped transmitted signals is also increased.

4.2 Multi-path Effects

Multipath effects are common in the indoor environment and they are difficult to deal with. As what we mentioned in Chapter 2.1, we use GCC-PHAT to estimate the time of arrival,

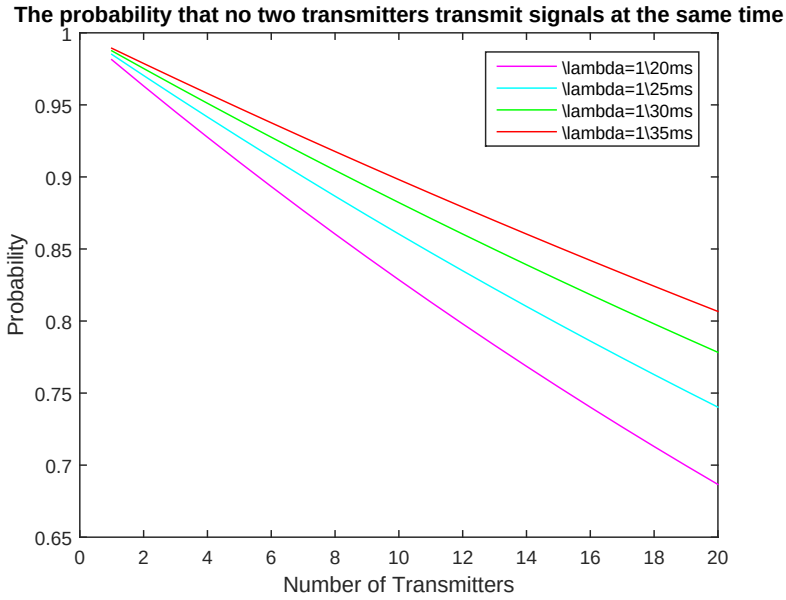

Figure 4.1: The probability of no overlapped transmitted signal

which proves to be robust to multipath effects. Compared with the generalized cross correlation method, GCC-PHAT applies the phase transformation for a sharp peak in the cross correlation function, which avoids the spreading from other paths. To conclude, GCC-PHAT can eliminate multipath effects and distinguish the time of arrival from the direct path.

4.3 Non-Line-of-Sight Scenarios

In indoor environments, non-line-of-sight caused by obstacles is a common problem. However, it will dramatically decrease the localization accuracy. The time of arrival from the direct path may be lost or masked by reverberations or noises. As a result, the estimated time of arrival from the direct path may be incorrect. Therefore, we need to make sure that the estimated time of arrival corresponds to the direct path.

We would like to exploit a method to decide whether an estimated time of arrival is associated with the true direct path through the information provided by GCC-PHAT. A reliability index is defined as the ratio between the energy of highest peak and the remaining samples,

$$\eta = \frac{\sum_{n \in D} R_{g_0 g_j}^{PHAT}(n)^2}{\sum_{n \notin D} R_{g_0 g_j}^{PHAT}(n)^2}, \tag{4.10}$$

where $D = [\hat{n} - n_D, \hat{n} + n_D]$ is an interval centered at the highest peak $\hat{n}$ of the generalized cross correlation function with the width equal to $2n_D + 1$. The energy of the direct path is expected to be inside the interval. Generally, the larger the reliability index is, the more

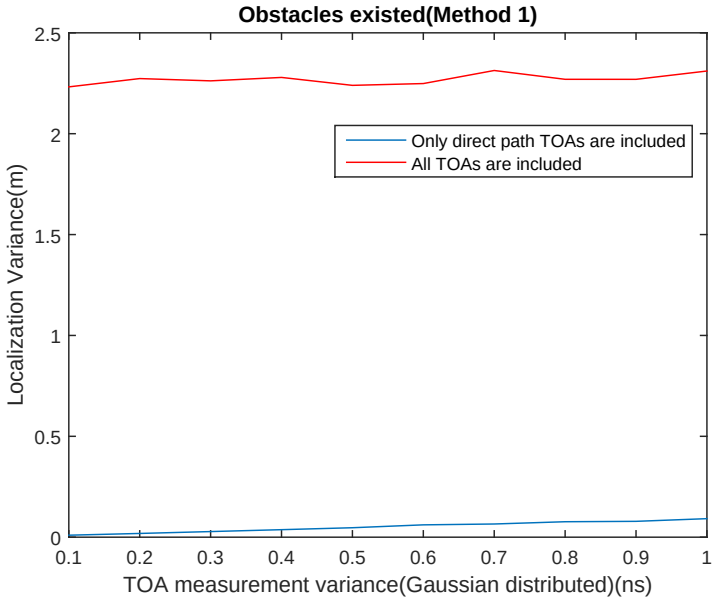

Figure 4.2: Non-line-of-sight scenarios

likely the estimated time of arrival is associated with the direct path. The reliability index is sent together with the corresponding TOA measurement. The TOA measurement is considered to be reliable and associated with the direct path if $\eta > \kappa\overline{\eta}$, where $\overline{\eta}$ is the average reliability index. κ is a threshold value, which is set with the trade-off between only keeping most reliable TOA measurements and keeping all TOA measurements [31].

We do a simulation to examine the changed accuracy when we discard the TOA measurements from the non-direct path. In a 6m$\times$4m room, eight receivers are placed uniformly. We use Method 1 (the centralized localization with the reference sensor 1) to compare the accuracy between only keeping the most reliable TOA measurements and keeping all TOA measurements. Suppose the receiver at $(6, 0)$ are blocked by obstacles, that is to say, the direct path from the transmitter to the receiver at $(6, 0)$ disappears. When we only keep the TOA measurements from the direct paths, we set κ equal to 0.9 and when we include all TOA measurements, we set κ equal to 0.1. The simulation result is shown in Figure 4.2.

From the simulation result, we can conclude that keeping the most reliable time of arrival measurements can achieve higher accuracy than including all time of arrival measurements.

4.4 Pruning incorrect TOA measurements

The true TOA measurements are easy to be masked in noisy indoor environments. Besides, the dynamic obstacles will mask the time of arrival from the direct path for some short time interval. Moreover, errors may occur during the time of arrival transmission. Since the incorrect time of arrival estimation will result in the wrong location estimation, it is

important to select a subset of the accurate measured TOAs for localization [32].

In a three-dimensional room, there are a set of I microphones and J acoustic events at unknown locations. The ith microphone and the jth source location is represented by vectors $\boldsymbol{r}_i$ and $\boldsymbol{s}_j$, respectively. Without loss of generality, we assume the speed of the signal is 1 and the internal delays and the onset time can be compensated. Let t_{ij} denote the observed TOA at the ith microphone to the jth acoustic event, which is given by

$$t_{ij} = \|r_i - s_j\| + \epsilon_{ij}, \tag{4.11}$$

where ϵ_{ij} denotes the measurement noise. Subtracting the square of equation (4.11) for $i = 1$ and $j = 1$, we obtain

$$-(\boldsymbol{r}_i - \boldsymbol{r}_1)^T(\boldsymbol{s}_j - \boldsymbol{s}_1) = 0.5(t_{ij}^2 - t_{1j}^2 - t_{i1}^2 + t_{11}^2), \tag{4.12}$$

for $i = 2, ..., I$ and $j = 2, ..., J$. With this, we can express it in the vector form,

$$-\overline{\boldsymbol{R}}\overline{\boldsymbol{S}}^T = \boldsymbol{T}, \tag{4.13}$$

where $\overline{\boldsymbol{R}}$ is the relative microphone location (to $\boldsymbol{r}_1$) matrix, $\overline{\boldsymbol{S}}$ is the relative acoustic event location (to $\boldsymbol{s}_1$) matrix and $\boldsymbol{T}_{i-1j-1} = 0.5(t_{ij}^2 - t_{1j}^2 - t_{i1}^2 + t_{11}^2)$ [32].

According to (4.13), if there is no error in TOA measurements, $\overline{\boldsymbol{R}}\overline{\boldsymbol{S}}^T$ is at most rank 3. This property can be used to find out the correct subset of TOA measurements [32].

For all I microphones, from J acoustic events, the TOA measurement set is denoted as S_J and all $J-1$ unique combinations of S_J is given by

$$U_{J-1} = \begin{pmatrix} S_J \\ J-1 \end{pmatrix}. \tag{4.14}$$

Take a specific combination u from U_{J-1} to construct $\boldsymbol{T}_u$ for $j = u$ and compute the error, which is defined as

$$e_u = \|\boldsymbol{T}_u\|_F^2 = \sum_{i=1}^{N_r} \sigma_i^2(\boldsymbol{T}_u), \tag{4.15}$$

where $N_r = \min(I-1, J-2)$ and $\sigma_i(\boldsymbol{T}_u)$ is the singular value of $\boldsymbol{T}_u$. If all TOA measurements are correct, the errors are close to equal and the minimum error can represent the most reliable TOA measurements if they are different. When no TOA measurement is correct, all errors are small but the maximum error is relatively large compared to the error of all correct TOA measurements. Therefore, the subset of TOA measurements can be selected as [32]

$$S_o = \begin{cases} arg\min_u var\{e_u\} & \text{if } \max e_u < \alpha \\ S_J & \text{otherwise} \end{cases}. \tag{4.16}$$

The iterative method to prune all erroneous TOA measurements is summarized in Algorithm 2 [32].

Algorithm 2 Pruning incorrect TOA measurements

1. For $n = 0, 1, J - J_{min}$
2. Generate the set of all possible combinations of the set S_{J-1}

$$U_{J-n+1} = \begin{pmatrix} S_J \\ J - n + 1 \end{pmatrix}$$

3. For each $u \in U_{J-n+1}$, construct $\boldsymbol{T}_u$ and compute the error.
4. Update the best TOA sets,

$$S_{J-n+1} = \begin{cases} arg\min_s e_u & \text{if } \min e_u / \max e_u < \alpha \\ S_{J-n} & \text{otherwise} \end{cases}$$

5. End if $S_{J-n+1} = S_{J-n}$

5 Conclusions

Global positioning system (GPS) has already achieved high accuracy in localization in outdoor environments. However, there is still no satisfactory system for indoor localization because of multipath effects, non-line-of sight scenarios. Indoor localization is of great importance in our daily life, like the hospital and supermarkets. We developed an accurate indoor localization system in this master thesis.

Low energy Bluetooth is getting to be one of the foundations of IoT and it is widely used around the world. In this thesis, we used low energy Bluetooth signals for indoor localization. Considering the accuracy, TDOA based techniques were chosen for indoor localization. Since the first part of Bluetooth signals is identical, we used this signal segment for localization. The sources broadcast GFSK modulated Bluetooth signals periodically. After the receiver receives the signal, we used GCC-PHAT to calculate the time delay between the transmitter and the receiver. GCC-PHAT proves to achieve sampling accuracy in indoor environments, which is essential to resist multipath effects. The receivers will communicate with each other to exchange its time delay information. We proposed four TDOA localization methods in this thesis, two centralized methods and two decentralized methods. We used PDMM to implement the decentralized localization methods. Moreover, we compared the accuracy of the four proposed methods. Experimental results showed that we can localize the source with an accuracy of less than one centimeter when the SNR is higher than 5dB. Furthermore, based on the Cramer-Rao lower bound, we examined the best way to place receivers in indoor environments. We proved a uniform angular array is the optimal sensor geometry. Besides, the proposed system can deal with multipath effects, NLOS scenarios and the incorrect time of arrival measurements. What's more, we derived the number of sources that we can accurately localize simultaneously in one indoor environment in the thesis.

To conclude, we have developed a relatively accurate indoor localization system and we can implement the localization method in a distributed way. Because of time limitation, I have not done any real experiment. Further works can focus on the real experiments and adding the synchronization errors among the receivers.

Appendix A

As shown in Chapter 3, $var(\hat{s_0}) \geq tr(FIM^{-1})$. Use the subscript "$full$" and "$nei$" to denote the full TOA measurement information and the neighboring TOA measurement information, respectively. We can get the Fisher information matrix with the full TDOA measurement information,

$$FIM_{full} = (\frac{\partial \boldsymbol{h}_{full}(s_0)}{\partial s_0})^T \boldsymbol{R}_{full}^{-1} \frac{\partial \boldsymbol{h}_{full}(s_0)}{\partial s_0}.$$

We want to compare the accuracy between using the neighboring information of receiver 1 and the full measurement information. Assume $\mathcal{N}_1$ is the set of the neighboring nodes of node 1 and $M_1 = |\mathcal{N}_1|$. The Fisher information matrix with the neighboring TDOA measurement information is derived as

$$FIM_{nei} = (\frac{\partial \boldsymbol{h}_{nei}(s_0)}{\partial s_0})^T \boldsymbol{R}_{nei}^{-1} \frac{\partial \boldsymbol{h}_{nei}(s_0)}{\partial s_0}.$$

The relationship between the full measurement matrix and the neighboring measurement matrix is expressed as

$$\frac{\partial \boldsymbol{h}_{nei}(s_0)}{\partial s_0} = \boldsymbol{X}_{tr} \frac{\partial \boldsymbol{h}_{full}(s_0)}{\partial s_0},$$
$$\boldsymbol{R}_{nei} = \boldsymbol{X}_{tr} \boldsymbol{R}_{full} (\boldsymbol{X}_{tr})^T.$$

where $\boldsymbol{X}_{tr}$ denotes the transformation matrix from the full measurement information to the neighboring measurement information. $\boldsymbol{X}_{tr} \in \mathcal{R}^{M_1 * (M-1)}$ is of the form that each row is unique with only one number 1 whose column position denotes the neighboring node number, and all other elements are number 0. With this, we arrive at

$$FIM_{nei} = (\boldsymbol{X}_{tr} \frac{\partial \boldsymbol{h}_{full}(s_0)}{\partial s_0})^T (\boldsymbol{X}_{tr} \boldsymbol{R}_{full} (\boldsymbol{X}_{tr})^T)^{-1} (\boldsymbol{X}_{tr} \frac{\partial \boldsymbol{h}_{full}(s_0)}{\partial s_0})$$

$$= (\frac{\partial \boldsymbol{h}_{full}(s_0)}{\partial s_0})^T (\boldsymbol{X}_{tr})^T ((\boldsymbol{X}_{tr})^T)^{-1} \boldsymbol{R}_{full}^{-1} (\boldsymbol{X}_{tr})^{-1} (\boldsymbol{X}_{tr}) (\frac{\partial \boldsymbol{h}_{full}(s_0)}{\partial s_0})$$

$$= (\frac{\partial \boldsymbol{h}_{full}(s_0)}{\partial s_0})^T \boldsymbol{R}_{full}^{-1} \frac{\partial \boldsymbol{h}_{full}(s_0)}{\partial s_0}$$

$$= FIM_{full}.$$

To conclude, using the neighboring TDOA measurement information instead of the full TDOA measurement information will not decrease the accuracy.

Bibliography

[1] I. Guvenc and C. C. Chong, "A survey on toa based wireless localization and nlos mitigation techniques," *IEEE Communications Surveys Tutorials*, vol. 11, pp. 107–124, rd 2009.

[2] R. Heusdens and N. Gaubitch, "Time-delay estimation for toa-based localization of multiple sensors," in *2014 IEEE International Conference on Acoustics, Speech and Signal Processing (ICASSP)*, pp. 609–613, May 2014.

[3] S. T. Birchfield and A. Subramanya, "Microphone array position calibration by basis-point classical multidimensional scaling," *IEEE Transactions on Speech and Audio Processing*, vol. 13, pp. 1025–1034, Sept 2005.

[4] C. N. Reddy and M. B. Sujatha, "Tdoa computation using multicarrier modulation for sensor networks," in *ISSN:2249-5789 CH Nagarjuna Reddy et al, International Journal of Computer Science & Communication Networks,Vol 1(1),September-October*, 2011.

[5] F. Jiang, Y. Kuang, and . strm, "Time delay estimation for tdoa self-calibration using truncated nuclear norm regularization," in *2013 IEEE International Conference on Acoustics, Speech and Signal Processing*, pp. 3885–3889, May 2013.

[6] R. Kaune, "Accuracy studies for tdoa and toa localization," in *Information Fusion (FUSION), 2012 15th International Conference on*, pp. 408–415, July 2012.

[7] P. Kuakowski, J. Vales-Alonso, E. Egea-Lpez, W. Ludwin, and J. Garca-Haro, "Angle-of-arrival localization based on antenna arrays for wireless sensor networks," *Computers & Electrical Engineering*, vol. 36, no. 6, pp. 1181 – 1186, 2010.

[8] C. Wu, Z. Yang, Y. Liu, and W. Xi, "Will: Wireless indoor localization without site survey," in *INFOCOM, 2012 Proceedings IEEE*, pp. 64–72, March 2012.

[9] C. Figuera, J. L. Rojo-lvarez, M. Wilby, I. Mora-Jimnez, and A. J. Caamao, "Advanced support vector machines for 802.11 indoor location," *Signal Processing*, vol. 92, no. 9, pp. 2126 – 2136, 2012.

[10] S. H. Fang and C. H. Wang, "A dynamic hybrid projection approach for improved wi-fi location fingerprinting," *IEEE Transactions on Vehicular Technology*, vol. 60, pp. 1037–1044, March 2011.

[11] V. Filonenko, C. Cullen, and J. Carswell, "Investigating ultrasonic positioning on mobile phones," in *Indoor Positioning and Indoor Navigation (IPIN), 2010 International Conference on*, pp. 1–8, Sept 2010.

[12] L. Mainetti, L. Patrono, and I. Sergi, "A survey on indoor positioning systems," in *Software, Telecommunications and Computer Networks (SoftCOM), 2014 22nd International Conference on*, pp. 111–120, Sept 2014.

[13] M. Z. Win, D. Dardari, A. F. Molisch, W. Wiesbeck, and J. Zhang, "History and applications of uwb [scanning the issue]," *Proceedings of the IEEE*, vol. 97, pp. 198–204, Feb 2009.

[14] Z. Song, G. Jiang, and C. Huang, "A survey on indoor positioning technologies," in *CH Nagarjuna Reddy et al, International Journal of Computer Science & Communication Networks,Vol 1(1),September-October 2011*, 2011.

[15] L. M. Ni, Y. Liu, Y. C. Lau, and A. P. Patil, "Landmarc: indoor location sensing using active rfid," in *Pervasive Computing and Communications, 2003. (PerCom 2003). Proceedings of the First IEEE International Conference on*, pp. 407–415, March 2003.

[16] Y. Chen, D. Lymberopoulos, J. Liu, and B. Priyantha, "Indoor localization using fm signals," *IEEE Transactions on Mobile Computing*, vol. 12, pp. 1502–1517, Aug 2013.

[17] J. Hallberg, M. Nilsson, and K. Synnes, "Positioning with bluetooth," in *Telecommunications, 2003. ICT 2003. 10th International Conference on*, vol. 2, pp. 954–958 vol.2, Feb 2003.

[18] "Bluetooth low energy white paper," June 2012.

[19] A. Kotanen, M. Hannikainen, H. Leppakoski, and T. D. Hamalainen, "Experiments on local positioning with bluetooth," in *Information Technology: Coding and Computing [Computers and Communications], 2003. Proceedings. ITCC 2003. International Conference on*, pp. 297–303, April 2003.

[20] https://en.wikipedia.org/wiki/Internet_of_things.

[21] J. Schmalenstroeer and R. Haeb-Umbach, "Investigations into bluetooth low energy localization precision limits," in *2016 24th European Signal Processing Conference (EUSIPCO)*, pp. 652–656, Aug 2016.

[22] dr.ir. Emanuel A.P. Habets, "Room impulse response generator," 2003.

[23] C. Knapp and G. Carter, "The generalized correlation method for estimation of time delay," *IEEE Transactions on Acoustics, Speech, and Signal Processing*, vol. 24, pp. 320–327, Aug 1976.

[24] R. Schiphorst, F. Hoeksema, and K. Slump, "Bluetooth demodulation algorithms and their performance," in *nd Karlsruhe Workshop on Software Radios*, pp. 99–106, 2002.

[25] A. H. Sayed, A. Tarighat, and N. Khajehnouri, "Network-based wireless location: challenges faced in developing techniques for accurate wireless location information," *IEEE Signal Processing Magazine*, vol. 22, pp. 24–40, July 2005.

[26] G. Zhang and R. Heusdens, "Distributed optimization using the primal-dual method of multipliers," *IEEE Transactions on Signal and Information Processing over Networks*, vol. PP, no. 99, pp. 1–1, 2017.

[27] B. Yang and J. Scheuing, "Cramer-rao bound and optimum sensor array for source localization from time differences of arrival," in *Proceedings. (ICASSP '05). IEEE International Conference on Acoustics, Speech, and Signal Processing, 2005.*, vol. 4, pp. iv/961–iv/964 Vol. 4, March 2005.

[28] K. W. Lui and H. So, "A study of two-dimensional sensor placement using time-difference-of-arrival measurements," *Digital Signal Processing*, vol. 19, no. 4, pp. 650 – 659, 2009.

[29] W. Meng, L. Xie, and W. Xiao, "Optimal sensor pairing for tdoa based source localization and tracking in sensor networks," in *Information Fusion (FUSION), 2012 15th International Conference on*, pp. 1897–1902, July 2012.

[30] S. Boyd, A. Ghosh, B. Prabhakar, and D. Shah, "Randomized gossip algorithms," *IEEE Transactions on Information Theory*, vol. 52, pp. 2508–2530, June 2006.

[31] A. Canclini, F. Antonacci, A. Sarti, and S. Tubaro, "Acoustic source localization with distributed asynchronous microphone networks," *IEEE Transactions on Audio, Speech, and Language Processing*, vol. 21, pp. 439–443, Feb 2013.

[32] N. D. Gaubitch, "Pruning incorrect toa measurements," 2014.